J|A|C|S
COMMUNICATIONS

Published on Web 10/21/2006

A Catalytic Nanomaterial-Based Optical Chemo-Sensor Array

Na Na, Sichun Zhang,* Shuai Wang, and Xinrong Zhang*

Department of Chemistry, Key Laboratory for Atomic and Molecular Nanosciences of the Education Ministry, Tsinghua University, 100084, Beijing, P. R. China

Received May 24, 2006; E-mail: sczhang@chem.tsinghua.edu.cn; xrzhang@chem.tsinghua.edu.cn

Cross-reactive chemical sensor arrays, known as "electronic noses" or "electronic tongues", are sensing systems that mimic the olfactory systems of animals. The central idea of cross-reactive chemical sensor arrays is to create sensing elements of the array with distinct but overlapping selective responses to a range of materials of interest, to generate a pattern that is discernibly different for each sample.[1] Existing sensing schemes exploit a variety of chemical interaction strategies including the use of modified tin oxides,[2] intrinsically conductive polymers and conductive polymer composites,[3] surface acoustic wave transducers coated with molecular reagents,[4] quartz crystal microbalances,[5] and dye-doped polymers[6] and other matrices.[7] Although the use of existing sensing mechanisms and already-developed data processing procedures have contributed much to improving the discrimination and recognition ability of the existing sensor arrays, the discovery of new sensing strategies and materials is still one of the most important factors that determine the development of this technique.

Chemiluminescence (CL) generated on the surface of solid materials is an interesting phenomenon which has been observed during the mixing of porous silicon with nitric acid or persulfate, and also in the agglomeration of copper or silver atoms in a matrix of noble gas atoms to form small clusters.[8] We have investigated the CL behaviors of many analytes on catalytic nanomaterials and developed a series of sensors for measuring alcohols, amines, thiols, and other gases or vapors.[9] Those compounds are oxidized catalytically by oxygen from the air on the surface of nanomaterials. The released energy of the catalytic reaction is absorbed by some of the reaction products, forming excited intermediates which decay from this excited-state to the ground state with light emission. The excited intermediates can also transfer their energy to dopant metal ions such as Eu^{3+} or Tb^{3+} in the catalytic nanomaterials, forming excited states of doped ions which relax by light emission.[10] The materials used to produce CL are not limited to traditional catalysts: even those which are not commonly thought of as catalysts, such as MgO and $SrCO_3$, have strong CL emission at nanoscale sizes. In addition, the morphological and structural differences of the catalytic nanomaterials lead to different CL responses.[11]

In the present study, we find that luminescent efficiencies of the CL are different for a given compound on different nanomaterials. As shown in Figure 1A, ethanol gives the strongest emission signal on ZrO_2/Tb^{3+} (ZrO_2 doped with 5% Tb^{3+}), while no signal is seen on nanosized WO_3 and Fe_2O_3. Hydrogen sulfide generates an obvious emission on WO_3, Fe_2O_3, and Y_2O_3, but no emission on others. Trimethylamine (TMA) produces strong signals on ZrO_2/Eu^{3+} (ZrO_2 doped with 5% Eu^{3+}), on Al_2O_3, and on ZrO_2/Tb^{3+}, but only weak signals on others. Similarly, the same nanomaterial exhibits different CL properties upon exposure to different analytes. A strong signal can be obtained on Fe_2O_3 for the detection of hydrogen sulfide, while there is only a weak response for TMA and no signal for ethanol (Figure 1A). On ZrO_2/Tb^{3+}, ethanol and TMA give bright luminescence, but hydrogen sulfide gives almost no luminescence.

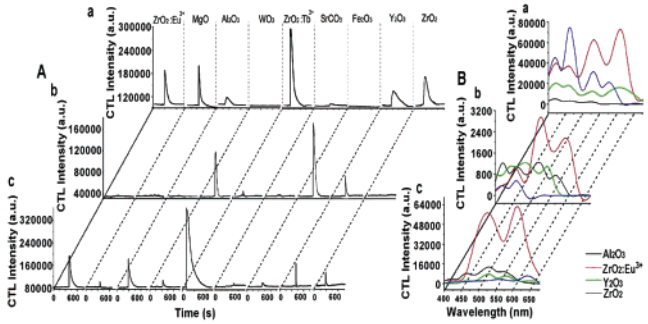

Figure 1. Chemo-selective response of CL on nanomaterials. (A) The fingerprint profiles of integrate CL intensity on nine nanomaterials for (a) ethanol, (b) hydrogen sulfide, and (c) TMA. The nanomaterials are, from left to right, ZrO_2/Eu^{3+}, MgO, Al_2O_3, WO_3, ZrO_2/Tb^{3+}, $SrCO_3$, Fe_2O_3, Y_2O_3, and ZrO_2. (B) A comparison of CL spectra on the sensing materials Al_2O_3, ZrO_2/Eu^{3+}, Y_2O_3, and ZrO_2 for (a) ethanol, (b) hydrogen sulfide, and (c) TMA.

The CL spectral shapes of a compound are different on various nanomaterials. As shown in Figure 1B, the spectral shape of ethanol is different on Al_2O_3, ZrO_2/Eu^{3+}, Y_2O_3, and ZrO_2. The peak emission of ethanol on ZrO_2/Eu^{3+} is at a wavelength of 620 nm, while that on Al_2O_3 is 425 nm. In the same way, the spectral shapes of different compounds on the same nanomaterial are also different, such as those of ethanol, hydrogen sulfide, and TMA shown in Figure 1B. The chemo-selective responses of CL on catalytic nanomaterials provide abundant optical information which motivates the fabrication of cross-reactive chemical sensor arrays.

For demonstration purposes, a 3×3 array of nine catalytic nanomaterials was fabricated on a ceramic chip with a temperature controller (Figure 2A). We examined three kinds of compounds, alcohols, amines, and thiols, to represent a wide range of chemical functionality. When the array is exposed to air without any sample, a blank image is recorded (Figure 2B-a). The CL images for ethanol, hydrogen sulfide, and TMA on the sensor array are distinct, as shown in Figure 2B-b,c,d. For example, ethanol is identified by its strong CL emission at spots 2,2 and 3,2, medium CL emission at 1,1, 1,2, and 3,3, and weak CL emission at 1,3 and 2,3. Hydrogen sulfide is identified by strong CL emission at spots of 3,1, medium CL emission at 2,1, and weak CL emission at 2,2 and 3,2, while TMA is identified by strong CL emission at 2,2, medium CL emission at 1,1, 1,3, and 3,2, and weak CL emission at spots 1,2, 2,1, 3,1, and 3,3. Therefore, a compound can be "fingerprinted" by the positions of the luminous spots and their relative CL intensities.

Though the present sensor array allows recognition of compounds of different chemical functionality as described above, the discrimination of compounds within a given chemical class remains a challenge. Here, we show the results for discrimination of four alcohols, namely methanol, ethanol, *n*-propanol, and *n*-butanol, with the CL sensor array. A comparison of images for the four alcohols

10.1021/ja063632f CCC: $33.50

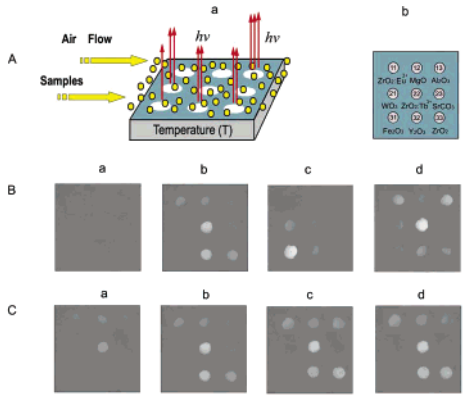

Figure 2. Schematic diagrams of the CL sensor array and the images recorded upon exposure to various samples. (A) Schematic diagrams of the CL sensor array (a) and the arrangement of nanomaterial spots (b). The sensor elements are arranged as follows: ZrO_2/Eu^{3+} (1,1), MgO (1,2), Al_2O_3 (1,3), WO_3 (2,1), ZrO_2/Tb^{3+} (2,2), $SrCO_3$ (2,3), Fe_2O_3 (3,1), Y_2O_3 (3,2), and ZrO_2 (3,3). (B) Images obtained by the sensor array after exposure to air for 1 min without any sample (a), with ethanol vapor (b), hydrogen sulfide (c), and TMA vapor (d). (C) Images obtained by the sensor array upon exposure to four alcohol vapors: (a) methanol, (b) ethanol, (c) *n*-propanol, and (d) *n*-butanol. The integrated CL intensities were recorded.

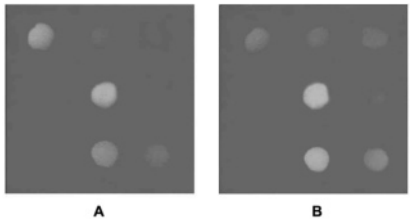

Figure 3. The impact of working temperature on the CL images of ethanol obtained by the sensor array: CL images of ethanol at the temperature of 190 °C (A) and 210 °C (B).

with the same concentration is shown in Figure 2C. Methanol and ethanol are easily distinguished from the others in these images. Though the luminous spots appeared at the same position (1,1, 1,2, 1,3, 2,2, 3,2, and 3,3) for *n*-propanol and *n*-butanol, their relative brightness is different. For example, spot 1,3 shows medium CL emission for *n*-propanol but weak CL emission for *n*-butanol.

The images of the sensor array can be adjusted by changing the working temperature, because the mechanisms and rates of catalytic reactions are dependent on temperature, which leads to different luminescence efficiencies and spectral shapes. The images of ethanol obtained on the array at 195 and 210 °C are shown in Figure 3A and B. New luminous spots emerge at the 2,3 position and the brightnesses of 1,2, 1,3, 2,2, 3,2, and 3,3 increase when the temperature is increased from 195 and 210 °C. At the same time, the brightness of 1,1 weakened. Furthermore, the brightness ratios of 1,1 to 3,3 and 2,2 to 3,2 clearly decrease. These results indicate that, even if similar images were recorded with the sensor array for two analytes at one temperature, they may be differentiated by means of images at another temperature.

The sensor array can also be used to quantify a given analyte by its CL emission intensity, because CL intensities vary linearly with analyte concentration. The linear range for the determination of ethanol is 45−550 ppm with a detection limit of 15 ppm on the ZrO_2/Eu^{3+} spot and 8.0−2000 ppm for hydrogen sulfide on Fe_2O_3 with a detection limit of 3.0 ppm. TMA on Y_2O_3 is linear from 60−42000 ppm with a detection limit of 10 ppm. It should be pointed out that the linear range and detection limit for each analyte vary significantly for different catalytic nanomaterials.

It is expected that the present sensor array could be extended to discrimination of samples in solution, since we have found that amino acids, saccharides, and steroid pharmaceuticals can produce CL emission on the surface of nanomaterials.[12] We are at present working to develop sensor arrays with more sensing elements and completing fabrication of an integrated device for the recognition and discrimination of real samples. We intend to apply this technique to the analysis of explosives and to volatile organic compounds in metabolic disorders.

Acknowledgment. This work is supported by grants from the NSFC (Grant Nos. 20575034, 20375022, and 20535020). We thank Prof. John Lewis at University of Arizona for the improvement of English usage. We also thank Dr. Zhenyu Zhang and Jinjun Shi for their constructive suggestions.

Note Added after ASAP Publication. In the version of this paper published ASAP on October 21, 2006, the incorrect panels of Figure 2B were cited in the fourth sentence of paragraph 5. The corrected version was published ASAP on October 23, 2006.

Supporting Information Available: Related experimental procedures and additional data. This material is available free of charge via the Internet at http://pubs.acs.org.

References

(1) (a) Albert, K. J.; Lewis, N. S.; Schauer, C. L.; Sotzing, G. A.; Stitzel, S. E.; Vaid, T. P.; Walt, D. R. *Chem. Rev.* **2000**, *100*, 2595−2626. (b) Rakow, N. A.; Suslick, K. S. *Nature* **2000**, *406*, 710−713. (c) Dickinson, T. A.; White, J.; Kauer, J. S.; Walt, D. R. *Nature* **1996**, *382*, 697−700.
(2) Su, M.; Li, S. Y.; Dravid, V. P. *J. Am. Chem. Soc.* **2003**, *125*, 9930−9931.
(3) Seyama, M.; Iwasaki, Y.; Ogawa, S.; Sugimoto, I.; Tate, A.; Niwa, O. *Anal. Chem.* **2005**, *77*, 4228−4234. (b) Kim, Y. S.; Ha, S. C.; Yang, Y.; Kim, Y. J.; Cho, S. M.; Yang, H.; Kim, Y. T. *Sens. Actuators, B* **2005**, *108*, 285−291.
(4) Santos, J. P.; Fernandez, M. J.; Fontecha, J. L.; Lozano, J.; Aleixandre, M.; Garcia, M.; Gutierrez, J.; Horrillo, M. C. *Sens. Actuators, B* **2005**, *107*, 291−295.
(5) Dickert, F. L.; Hayden, O.; Zenkel, M. E. *Anal. Chem.* **1999**, *71*, 1338−1341.
(6) (a) Greene, N. T.; Shimizu, K. D. *J. Am. Chem. Soc.* **2005**, *127*, 5695−5700. (b) Song, L. N.; Ahn, S.; Walt, D. R. *Anal. Chem.* **2006**, *78*, 1023−1033. (c) Michael, K. L.; Taylor, L. C.; Schultz, S. L.; Walt, D. R. *Anal. Chem.* **1998**, *70*, 1242−1248. (d) Bencic-Nagale, S.; Walt, D. R. *Anal. Chem.* **2005**, *77*, 6155−6162.
(7) (a) Rakow, N. A.; Sen, A.; Janzen, M. C.; Ponder, J. B.; Suslick, K. S. *Angew. Chem., Int. Ed.* **2005**, *44*, 4528−4532. (b) Zhang, C.; Suslick, K. S. *J. Am. Chem. Soc.* **2005**, *127*, 11548−11549.
(8) (a) McCord, P.; Yau, S. L.; Bard, A. J. *Science* **1992**, *257*, 68−69. (b) König, L.; Rabin, I.; Schulze, W.; Ertl, G. *Science* **1996**, *274*, 1353−1355.
(9) (a) Zhu, Y. F.; Shi, J. J.; Zhang, Z. Y.; Zhang, C.; Zhang, X. R. *Anal. Chem.* **2002**, *74*, 120−124. (b) Zhang, Z. Y.; Xu, K.; Xing, Z.; Zhang, X. R. *Talanta* **2005**, *65*, 913−917. (c) Zhang, Z. Y.; Jiang, H. J.; Xing, Z.; Zhang, X. R. *Sens. Actuators, B* **2004**, *102*, 155−161. (d) Zhang, Z. Y.; Zhang, C.; Zhang, X. R. *Analyst* **2002**, *127*, 792−796.
(10) Zhang, Z. Y.; Xu, K.; Baeyens, W. R. G.; Zhang, X. R. *Anal. Chim. Acta* **2005**, *535*, 145−152.
(11) Sun, Z. Y.; Yuan, H. Q.; Liu, Z. M.; Han, B. X.; Zhang, X. R. *Adv. Mater.* **2005**, *17*, 2993−2997.
(12) (a) Lv, Y.; Zhang, S. C.; Liu, G. H.; Huang, M. W.; Zhang, X. R. *Anal. Chem.* **2005**, *77*, 1518−1525. (b) Huang, G. M.; Lv, Y.; Zhang, S. C.; Yang, C. D.; Zhang, X. R. *Anal. Chem.* **2005**, *77*, 7356−7365.

JA063632F